Bulletin of the Earthquake
Research Institute
University of Tokyo
Vol. 61 (1986) pp. 251-267

Report on DELP 1984 Cruises in the Middle Okinawa Trough Part IV: Heat Flow Measurements

Makoto YAMANO[1], Seiya UYEDA[1], Hajimu KINOSHITA[2] and Thomas W. C. HILDE[3],

1) Earthquake Research Institute, University of Tokyo
2) Department of Earth Sciences, Chiba University
3) Department of Geophysics, Texas A and M University

(Received April 18, 1986)

Abstract

New heat flow values were obtained at 17 sites in the middle Okinawa Trough by means of an Ewing type multiple-penetration device on the DELP-84 WAKASHIO cruise. The most remarkable finding was the extremely high heat flow (up to about 1600 mW/m^2) in a small depression called the Matsushima-84 Deep at the axis of the trough. The high and variable heat flow and non-linear temperature gradients observed in the depression indicate high hydrothermal activity.

1. Objectives

The Okinawa Trough is thought to be formed by recent back-arc spreading. The southwestern part of the trough is in a relatively advanced stage of spreading but the northeastern part appears to be still in a pre-spreading stage and the middle part in a nascent speading or rifting stage. The heat flow values formerly measured in the Okinawa Trough are rather high, supporting the young age of this basin (*e. g.* LU *et al.*, 1981). However, no general pattern of heat flow distribution can be clearly seen, though Vander Zouwen (1984) proposed that there is a high heat flow area near 126°E. Through the work on the DELP-84 WAKASHIO cruise, we intended to add more heat flow data to investigate the thermal evolution of the Okinawa Trough.

Another objective of heat flow measurement on the DELP-84 WAKASHIO cruise was to examine the existence of hydrothermal activity in the Okinawa Trough. Hydrothermal circulation was proposed to explain the fact that the observed heat flows on mid-ocean ridges and their flanks are variable and lower than expected from theoretical thermal

models (LISTER, 1972). Active hydrothermal vents were actually discovered by submersible observations at spreading centers in the eastern Pacific (*e. g.* CORLISS *et al.*, 1979). In the Mariana Trough, where active back-arc spreading is occurring, detailed heat flow surveys indicated extensive hydrothermal circulation (HOBART *et al.*, 1979). As the Okinawa Trough is also a young back-arc basin, we expected that similar hydrothermal circulations might be observed with closely spaced heat flow measurements using a multiple penetration type instrument.

3. Measurement Techniques

We used an Ewing type probe for geothermal gradient measurements. It can be used either as a 450 kg, 4.5m probe or as a 150 kg, 3m probe. Six thermistors were mounted in outrigger fashion along the lance which was strong enough to permit multiple penetrations. This recording system was made by Lamont-Doherty Geological Observatory of Columbia University. The resistance of thermistors and instrument tilt were recorded on a cassette magnetic tape. They were also telemetered by 12 kHz acoustic pulses to the surface ship, so that we could monitor the real-time measured temperatures and the attitude of the probe by the ship's ordinary echo-sounder. At the beginning of the cruise, the temperature records were very erratic and the acoustic pulses could not be clearly monitored. These problems were proven to be due to bad insulation of an underwater connector and the exhaustion of rechargeable batteries. After making improvements, we could obtain good temperature records and monitor the data on board.

The resolution of temperature variation by this instrument was about 0.0008°C, though the absolute accuracy of thermistor temperatures was about 0.1°C. We held the probe at several tens of meters above the sea floor for 5 to 10 minutes before every penetration. These temperature records were treated as the reference points for temperature measurements in the sediments. The bottom water temperature variation along the probe was negligible and the accuracy of temperature differences among thermistors was estimated to be 0.001 to 0.002°C.

The temperature variations of thermistor probes after the penetration are described by a function derived by Bullard (1954). The thermistors of our instrument were encased in 3.5 mm diameter stainless steel tubes, so that the thermal time constant in the sediment was 10 to 20 sec. For such a short thermal time constant, this function can be approximated by the inverse of time after penetration. We calculated the equilibrium temperature assuming that the temperature decay was inversely proportional to time. Fig. IV-1 shows an example of temperature-time records

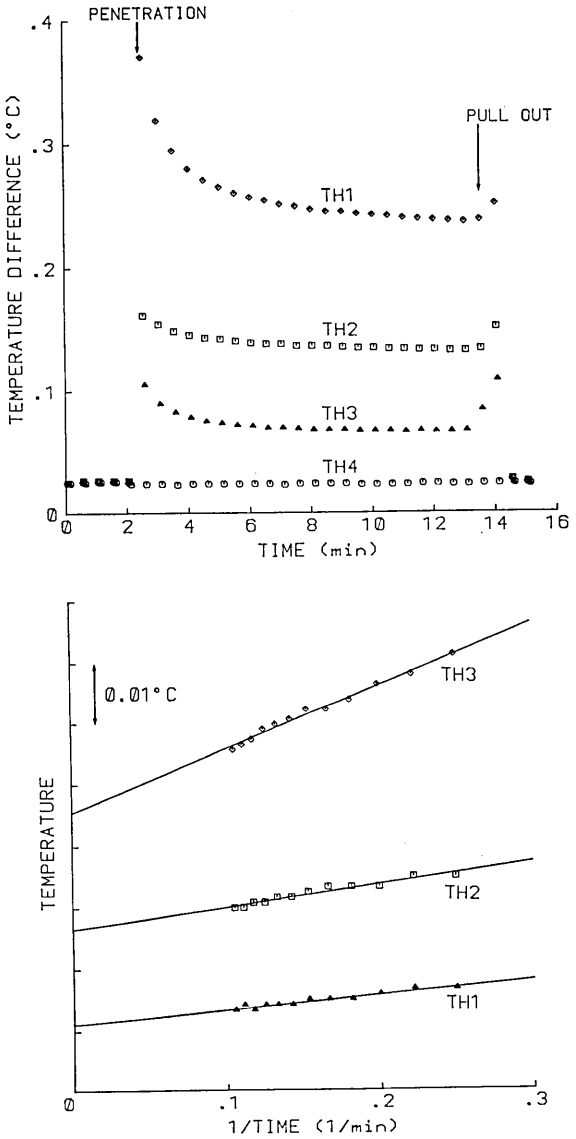

Fig. IV-1 (a). Temperature-time records at HF 6 H. Origin of the ordinate is arbitrary. Thermistor TH 4 did not penetrate into the sediment. (b) Measured temperatures versus reciprocal time after penetration at HF 6 H. Solid lines show extrapolation to the equilibrium.

obtained on this cruise and extrapolation of temperature to the equilibrium. The error in the calculation of equilibrium temperature, which includes the error due to uncertainty in the time of penetration, was generally 0.003 to 0.004°C. Thus, the total error in the equilibrium

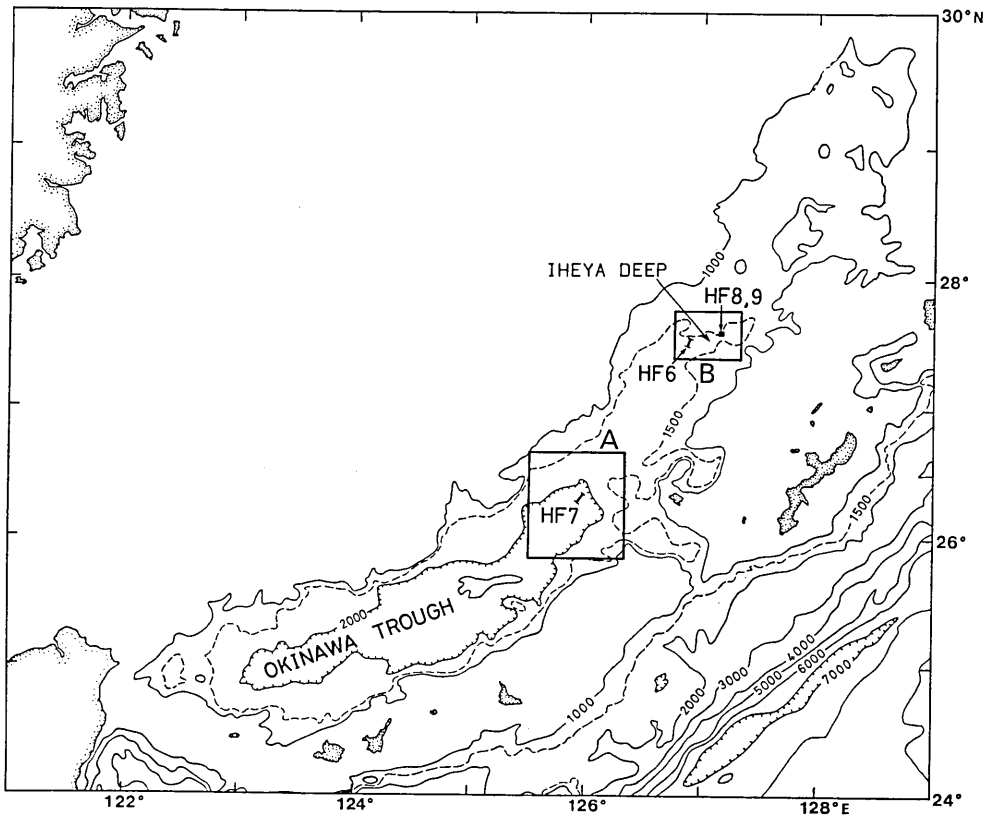

Fig. IV-2. Locations of heat flow stations. Detailed maps of areas A and B are shown in Figs. IV-3 and IV-5.

temperature in the mud relative to the bottom water temperature was estimated to be 0.004 to 0.006°C. In some cases, the temperature records of one or two thermistors were unstable, so that the error reached 0.01 to 0.02°C.

Thermal conductivities were measured on gravity core samples by the needle probe method (VON HERZEN and MAXWELL, 1959). The values obtained on board were corrected to in situ temperature and pressure conditions according to RATCLIFFE (1960).

3. Heat Flow Measurement Locations

We made heat flow measurements at four stations listed in Table IV-1. Alphabetic suffixes are used to distinguish multiple penetrations. The locations of the stations are shown in Fig. IV-2.

Table IV-1. Results of heat flow measurements

Station	Latitude N	Longitude E	D m	PEN m	N	G mK/m	K W/m K	Q_c mW/m²	Q_a mW/m²	V 10^{-8}m/s
HF 6A	27°29.3′	126°51.8′	1660	1.7	4	181	0.84*	152	93	10.9
6B	27°29.4′	126°51.9′	1650	1.0	2	(160)	0.84*	(135)		
6D	27°31.7′	126°53.3′	1670	2.7	5	100	0.84*	84		
6F	27°32.0′	126°53.6′	1690	0.7	2	(54)	0.84*	(46)		
6H	27°32.4′	126°53.7′	1660	1.5	3	154	0.84*	(130)	(48)	18.3
HF 7B	26°16.4′	125°55.2′	2110	1.6	4	224	1.01	227		
7C	26°17.3′	125°55.6′	2100	1.6	4	143	1.01	145		
7D	26°17.3′	125°55.5′	2100	1.6	4	129	1.01	130	153	−5.1
7E	26°20.2′	125°58.4′	2120	1.5	3	325	1.01	328		
7G	26°20.6′	125°58.4′	2150	2.4	4	263	1.01	266	388	−6.8
HF 8A	27°35.3′	127°09.5′	1760	4.9	3	474	0.84	398		
8B	27°35.4′	127°09.8′	1760	1.5	2	(978)	0.84	(822)		
HF 9A	27°35.2′	127°08.6′	1780	1.4	2	(1883)	0.84	(1581)		
9B	27°35.3′	127°08.6′	1780	2.3	3	1508	0.84	1267		
9C	27°35.4′	127°08.6′	1770	4.2	5	774	0.84	650	392	3.9
9D	27°35.1′	127°09.0′	1780	2.3	3	973	0.84	817	697	2.1
9E	27°35.7′	127°09.1′	1720	1.5	2	(53)	0.84	(46)		
GC 2	26°22.0′	125.59.7′	2150	1.0			1.01			
3	27°35.2′	127°08.6′	1780	1.0			0.84			

D is the water depth on the assumption that sound velocity is 1500 m/s; PEN is the estimated penetration of the lowermost active thermistor or the length of the obtained core; N is the number of active thermistors in mud; G is the temperature gradient; K is the thermal conductivity (* represents values measured at nearby stations); Q_c is the heat flow calculated by the conductive model; Q_a is the heat flow calculated by the advective model; V is the estimated vertical water flux (positive downward). Values in parentheses are less reliable.

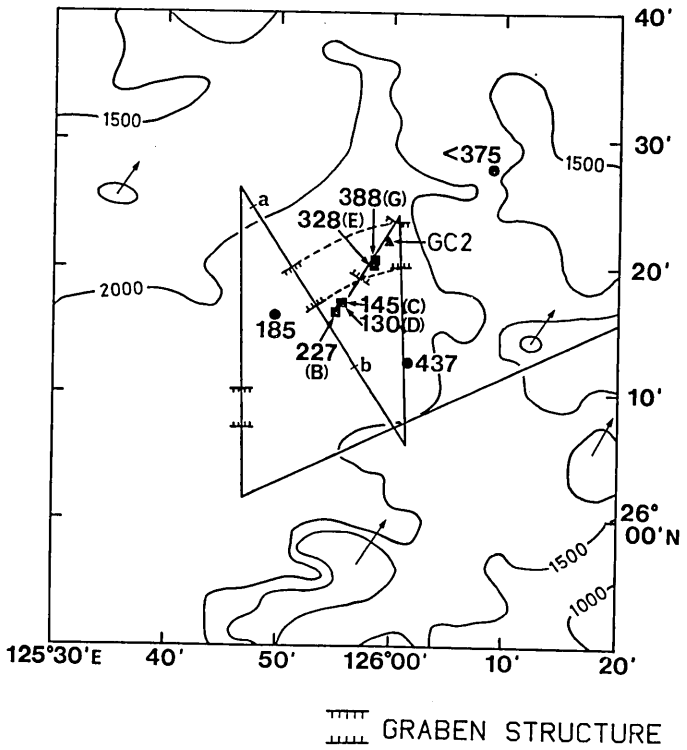

Fig. IV-3. Detailed bathymetry map of area A in Fig. IV-2. Solid lines are tracks of this cruise. Profile a-b is shown in Fig. IV-4. Heat flow values are given in mW/m² (squares; this cruise, circles; former measurements). Triangle marks location of gravity core sampling.

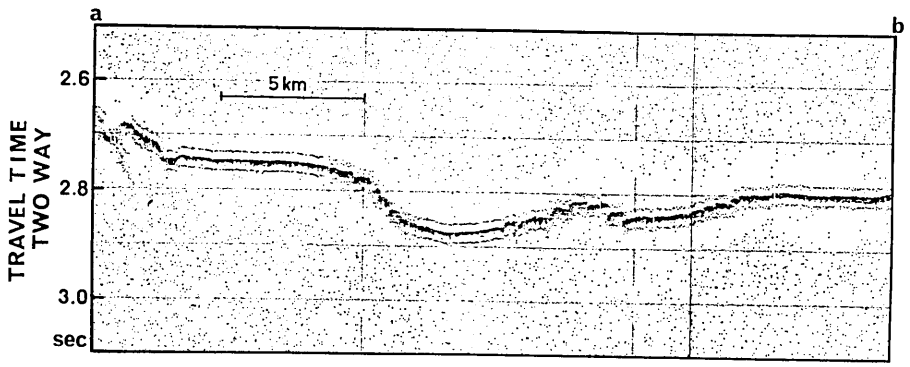

Fig. IV-4. 12 kHz echo-sounder record along the line a-b in Fig. IV-3.

The station HF 7 is located in the high heat flow area of VANDER ZOUWEN (1984) where all of four previously reported values exceed 180 mW/m² (Figs. IV-3 and IV-10). She stated that the high heat flow may be associated with a major north-south trending transform fault at about

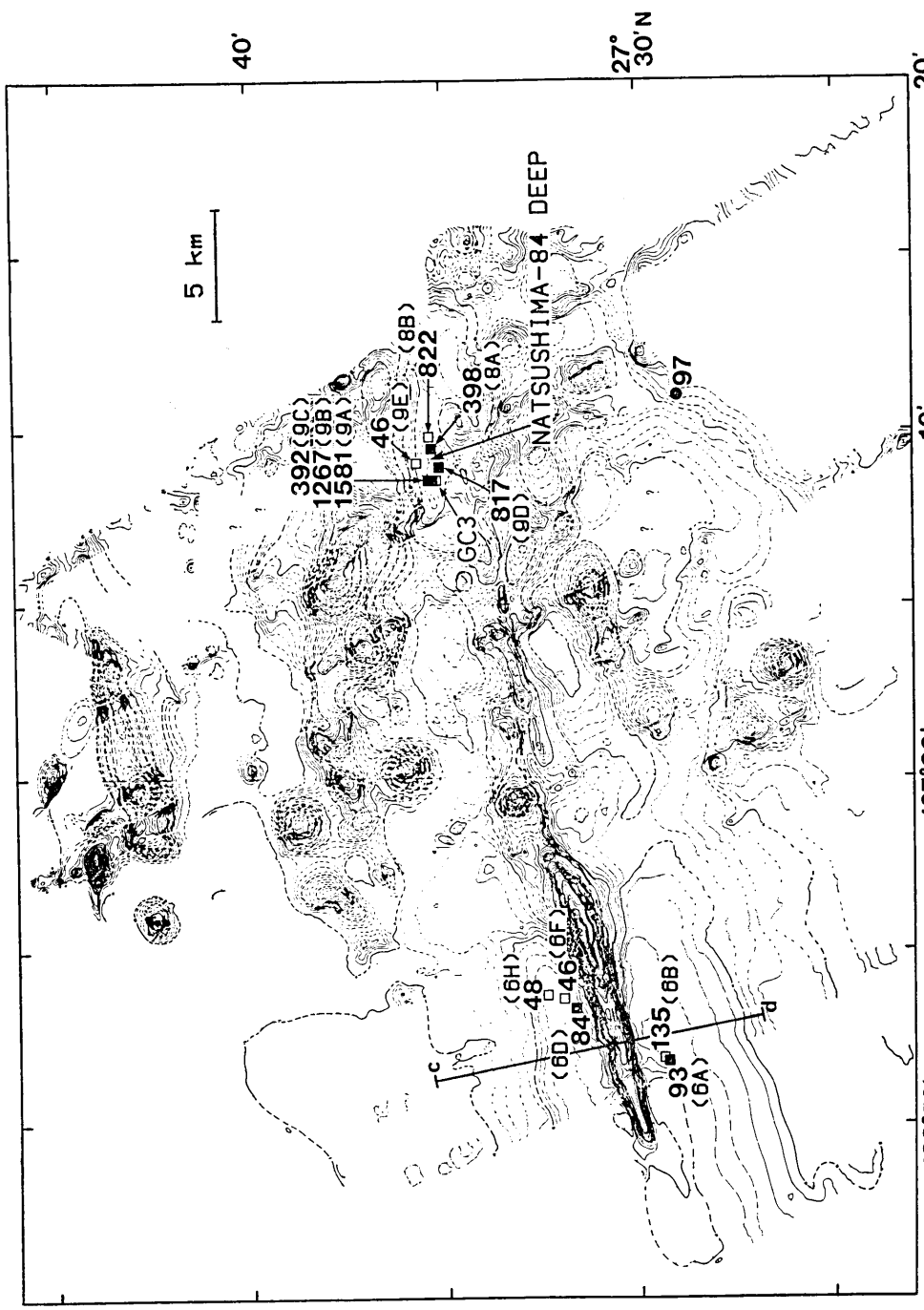

Fig. IV-5. Seabeam bathymetry map by R/V JEAN CHARCOT (SIBUET *et al.*, 1986) and heat flow values in mW/m^2 (squares; this cruise, circle; former measurement). Profile c-d is shown in Fig. IV-6.

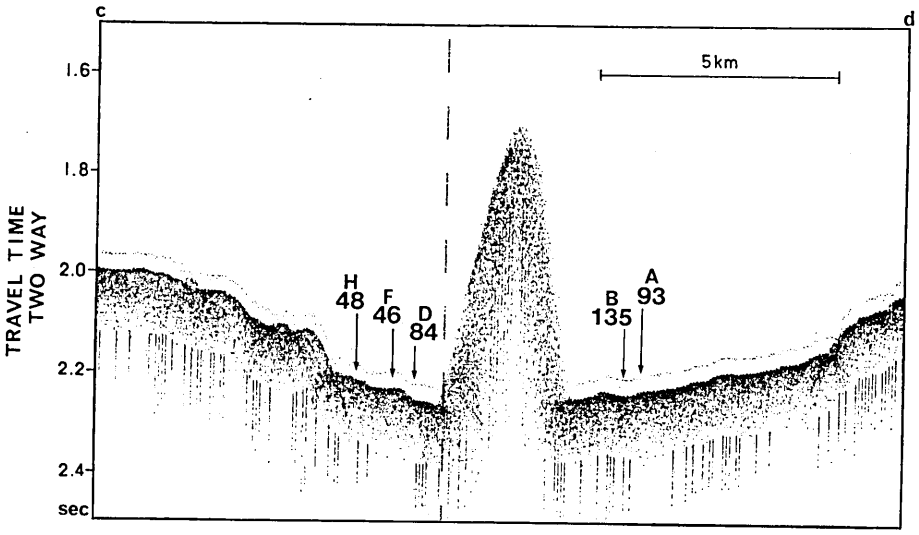

Fig. IV-6. Locations of HF 6 projected onto 12 kHz echo-sounder profile c-d in Fig. IV-5. Heat flow in mW/m².

126°E. The survey on this cruise suggests that the topography around HF 7 is relatively flat but there is a small graben structure extending east-west (Fig. IV-3). Fig. IV-4 is one of the 12 kHz echo-sounder profiles showing the graben. Heat flow measurements were carried out in the area to the south and inside of the graben (squares in Fig. IV-3).

The stations HF 6, HF 8, and HF 9 are sited along the inferred spreading center of the Okinawa Trough in the area called the Iheya Deep in this report (Fig. IV-2). Shortly after this cruise, R/V JEAN-CHARCOT made a survey of this area with the seabeam system and constructed a bathymetry map (Fig. IV-5, SIBUET *et al.*, 1986). There is an east-west striking ridge in the western part of the map. We measured heat flow in the sedimented basins on both sides of this ridge (HF 6). The positions of successful penetrations are projected onto the echo-sounder profile across the ridge in Fig. IV-6. HF 8 and HF 9 are located within a depression called the Natsushima-84 Deep which is about 1 km wide, 3 km long and surrounded by small seamounts (Fig. IV-5). This is the spot where the submersible SHINKAI-2000 made four dives after this cruise (UYEDA *et al.*, 1985). The position of each penetration in the depression is not well determined because of poor navigation by Loran *C* in this area. We believe, however, that the relative positions among penetration are fairly reliable.

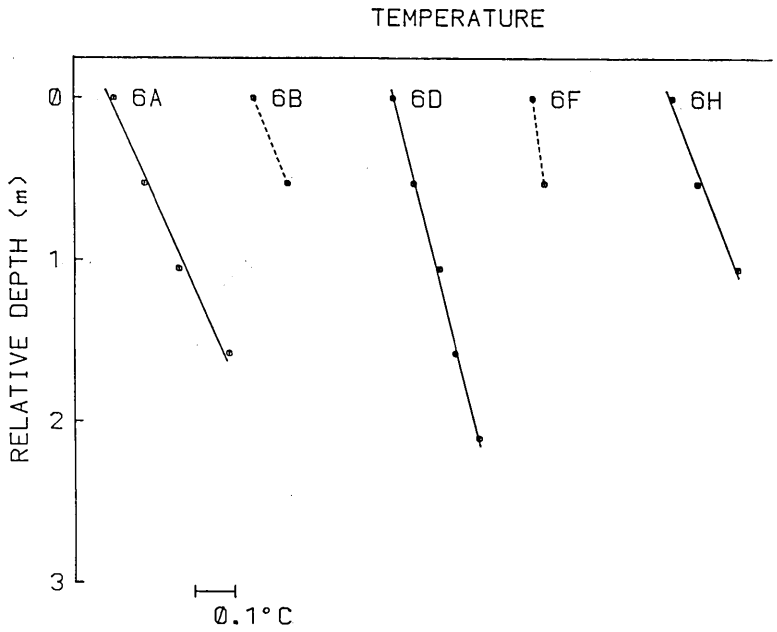

Fig. IV-7. (a) HF6

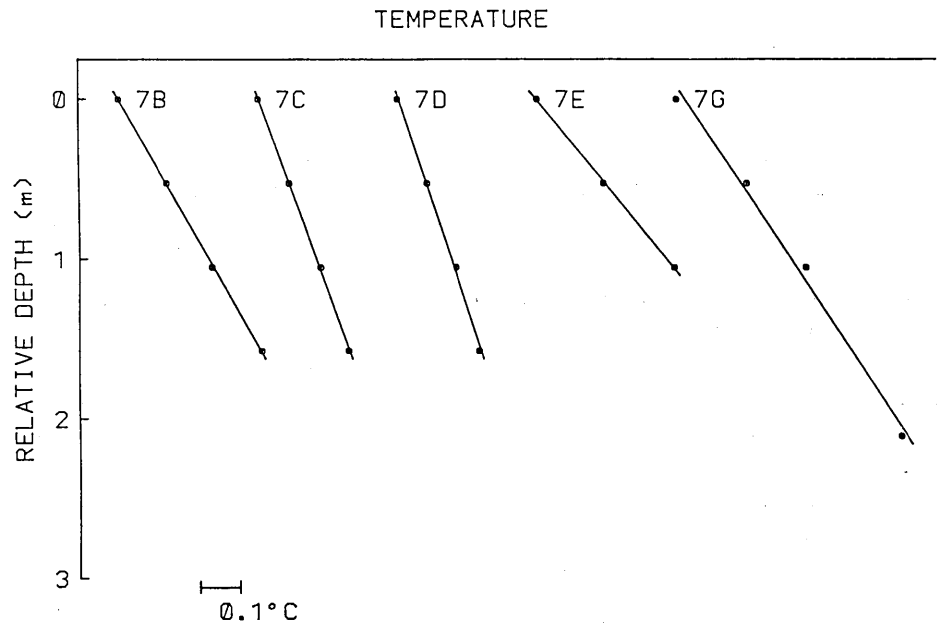

Fig. IV-7. (b) HF7

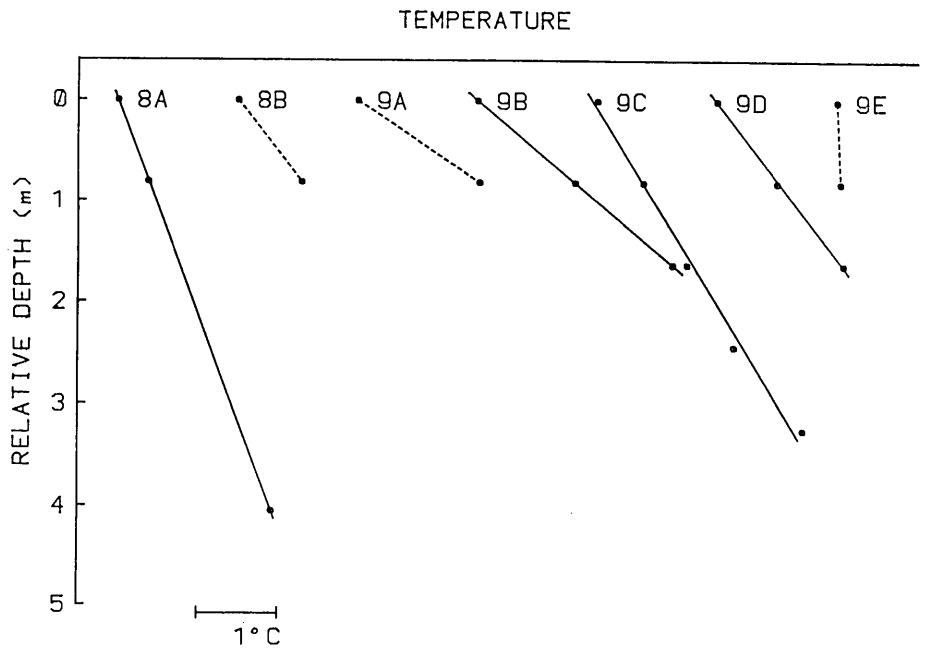

Fig. IV-7. (c) HF8 and 9

Fig. IV-7. Temperature versus depth profiles. Solid lines are the least squares fits by straight lines.

4. Results

We used the 3m probe at stations HF6 and HF7 and the 4.5m probe at HF8 and HF9. Seventeen penetrations were successful. The obtained temperature versus depth profiles are presented in Fig. IV-7. The penetration depth of the lowermost active thermistor in Table IV-1 was estimated from the temperature profile and the bottom water temperature measured after pulling out. At HF8B and HF9A through *D*, the probe penetrated fully into the sediments. The temperature of the lower thermistors, however, was higher than the instrument could record owing to very high temperature gradients, and therefore the data of these thermistors are missing in Fig. IV-7. In some cases (*e.g.* HF8A), temperature data are missing due to a breakdown of connections between thermistors and the recorder. The numbers of active thermistors in the mud in Table IV-1 do not include such thermistors.

Gravity core samples were taken near HF7 (GC2) and HF9 (GC3). The locations of sampling are listed in Table IV-1 and shown in Figs. IV-3 and IV-5. Fig. IV-8 shows the measured thermal conductivities plotted versus depth. Conductivity values from GC2 are rather scattered

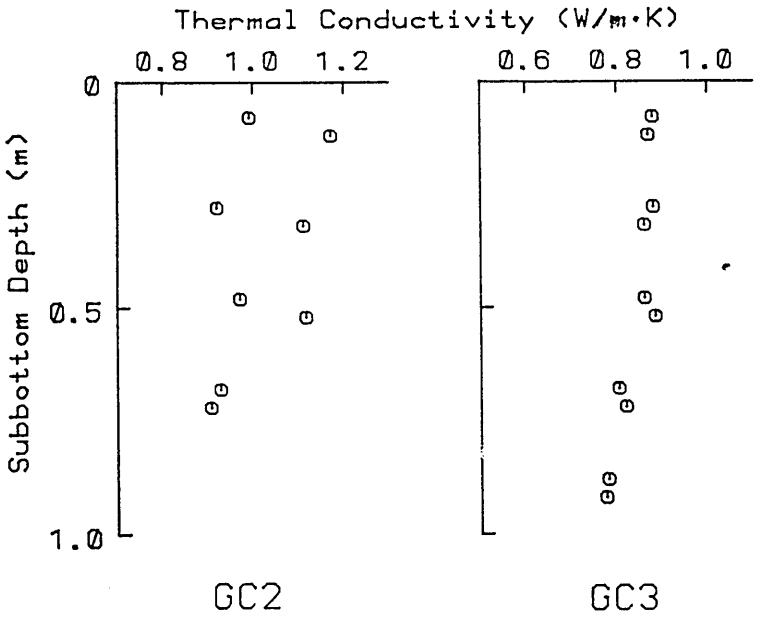

Fig. IV-8. Thermal conductivity versus depth measured on gravity core samples.

probably due to variations in the mineral composition and imperfect contact between the needle probe and the sediment. The mean value, 1.01 ± 0.10 W/m K, falls within the values reported around HF7, 0.83 to 1.12 W/m K. The conductivity profile of GC3 seems to show a slight decrease with depth. But the length of core,, 1m, is short compared to the length of the probe and the conductivity may increase in deeper sediments owing to compaction. Therefore, the decrease is not taken into account in the following calculations of heat flow and the mean value, 0.84 ± 0.04 W/m K, is used. We could not take core samples at HF6 and no thermal conductivity data was available in the vicinity. 0.84 W/m K at HF9 is used below.

Temperature gradients were determined by the least-squares fit to a straight line, though some of the temperature-depth profiles appear non-linear. The solid lines in Fig. IV-7 represent the best fitted gradients. The broken lines mean that the gradients are determined from only two thermistors and are less reliable. The product of the thermal conductivity and the linear temperature gradient gives heat flow by the conductive model in Table IV-1. Errors in the heat flow values are about 15% for the penetrations with linear temperature profiles.

5. Non-linear Temperature Profiles

Some of the temperature profiles are non-linear as mentioned above (e.g. HF 6 A, HF 7 G). Among many mechanisms which can cause such non-linear gradients, the most probable is the vertical pore water advection. Since the Okinawa Trough is a young marginal basin, it is likely that hydrothermal convections exist and pore water is flowing through the sediments. Here we use the model by BREDEHOEFT and PAPADOPULOS (1965) to interpret the non-linearity of temperature profile. Assuming that the flow of heat and fluid is vertical and steady, the temperature variation with depth is expressed as

$$T(z)=(T_L-T_U)\frac{e^{\beta z/L}-1}{e^{\beta}-1}+T_U \qquad \text{(IV-1)}$$

where

z=depth from the uppermost thermistor in the sediment;
T_L=temperature of the lowermost thermistor;
T_U=temperature of the uppermost thermistor in the sediment;
$\beta=v\rho CL/k$;
v=flow rate of the fluid (positive downward);
ρ=density of the fluid;
C=specific heat of the fluid;
k=thermal conductivity of the sediment;
L=vertical distance between the lowermost and uppermost thermistors in the sediment.

The non-linear temperature profiles were fitted to the equation (IV-1) by the method of least squares. The best fit curves are shown in Fig. IV-9. The total heat flow which is the sum of conductive heat flow and advective heat flow is

$$Q=k\frac{dT}{dz}-v\rho CT(z) \qquad \text{(IV-2)}$$

It should be noted that T in this equation is the temperature difference from the bottom water temperature. Using (IV-1), (IV-2) can be rewritten as

$$Q=\frac{k\beta}{L}\left(\frac{T_L-T_U}{e^{\beta}-1}-T_U\right) \qquad \text{(IV-3)}$$

The total heat flow by the advective model in Table IV-1 was calculated through (IV-3). We can also calculate the flow rate of pore water from the best fit β. Positive values mean that water is flowing downward. It

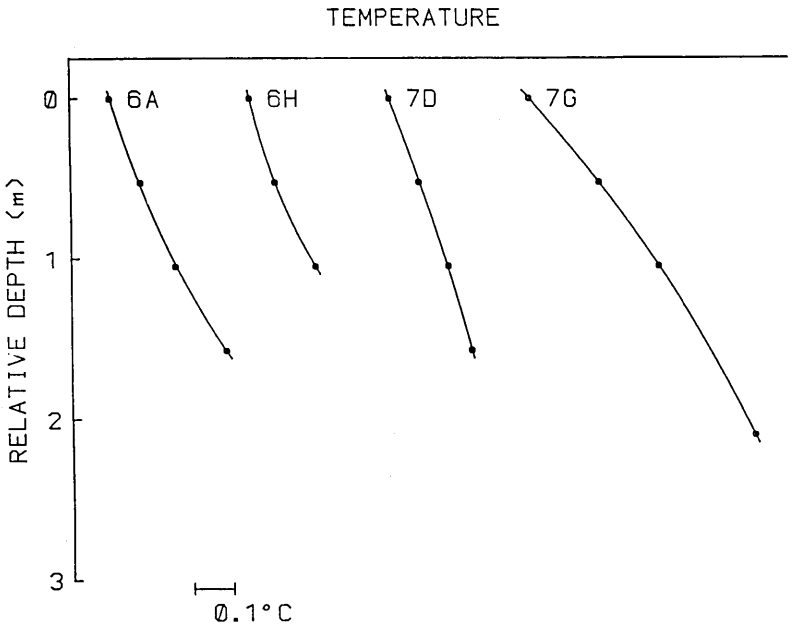

(a) HF 6 and 7

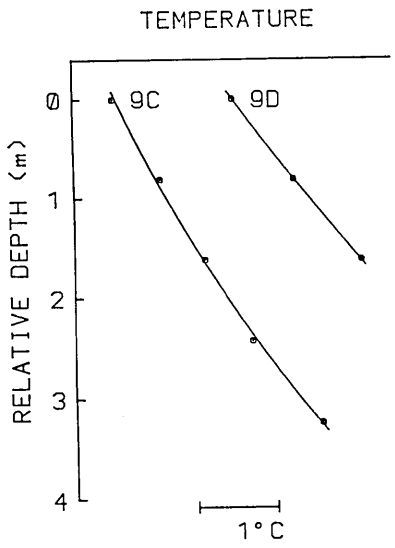

(b) HF 9

Fig. IV-9. Non-linear temperature profiles. Curves are the best fits by the pore water advection model.

is difficult to estimate the error in the total heat flow and flow rate because of the small number of data points and the shallow penetration depth.

Change in the bottom water temperature also may give non-linear temperature profiles. For example, we can explain the profile at HF7G by a sudden bottom temperature decrease of 0.15°C nine days before the measurement. An annual variation with an amplitude of 0.27°C can also fit the data. Although there are not enough hydrographic data to examine the stability of the bottom water temperatures in the studied area, temperature variations of this magnitude may not be impossible. However, both linear and non-linear temperature profiles are observed in close proximity, suggesting that the non-linearity is not caused by a change in the bottom water temperature. Moreover, the temperature profile at HF9C requires anomalous amounts of change in water temperature, a sudden increase of 0.78°C or annual oscillation with an amplitude of 2.4°C.

Variation of thermal conductivity with depth should be considered as well. Unfortunately, there is no conductivity data for the sediments deeper than 1m. But the rates of conductivity variations necessary for the observed non-linearity are extremely high, 40 to 60%, and this mechanism also cannot explain the coexistence of linear and non-linear profiles. Therefore, variation of conductivity does not seem to be the main cause of the non-linear temperature profiles.

6. Heat Flow Distributions

The obtained heat flows are plotted in Figs. IV-3, IV-5 and IV-6. We took the total heat flow by the advective model for HF6A, 6H, 7G, and 9C, and the conductive heat flow for other penetrations. At HF7D and 9D, the conductive heat flow values were used, because the temperature profiles can also well be fitted to a straight line and the non-linearity may result from errors in temperature measurements and/or variation of thermal conductivity. In these two cases, differences between the calculated conductive and total heat flow values are about 15%. Fig. IV-10 shows all the heat flow measurements in the southern and middle Okinawa Trough area. The data by HERMAN *et al.* (1978) and LU *et al.* (1981) and some unpublished data are added to the compilation by YOSHII (1979).

All of five heat flow values at HF7 are higher than 130 mW/m^2. It supports the idea of a high heat flow area by VANDER ZOUWEN (1984), though it is not clear whether this high heat flow is related to a transform fault. No transform fault was found in this region. Heat flows in the studied small graben appear higher than outside the graben (Fig. IV-3). More data is necessary to ascertain the difference.

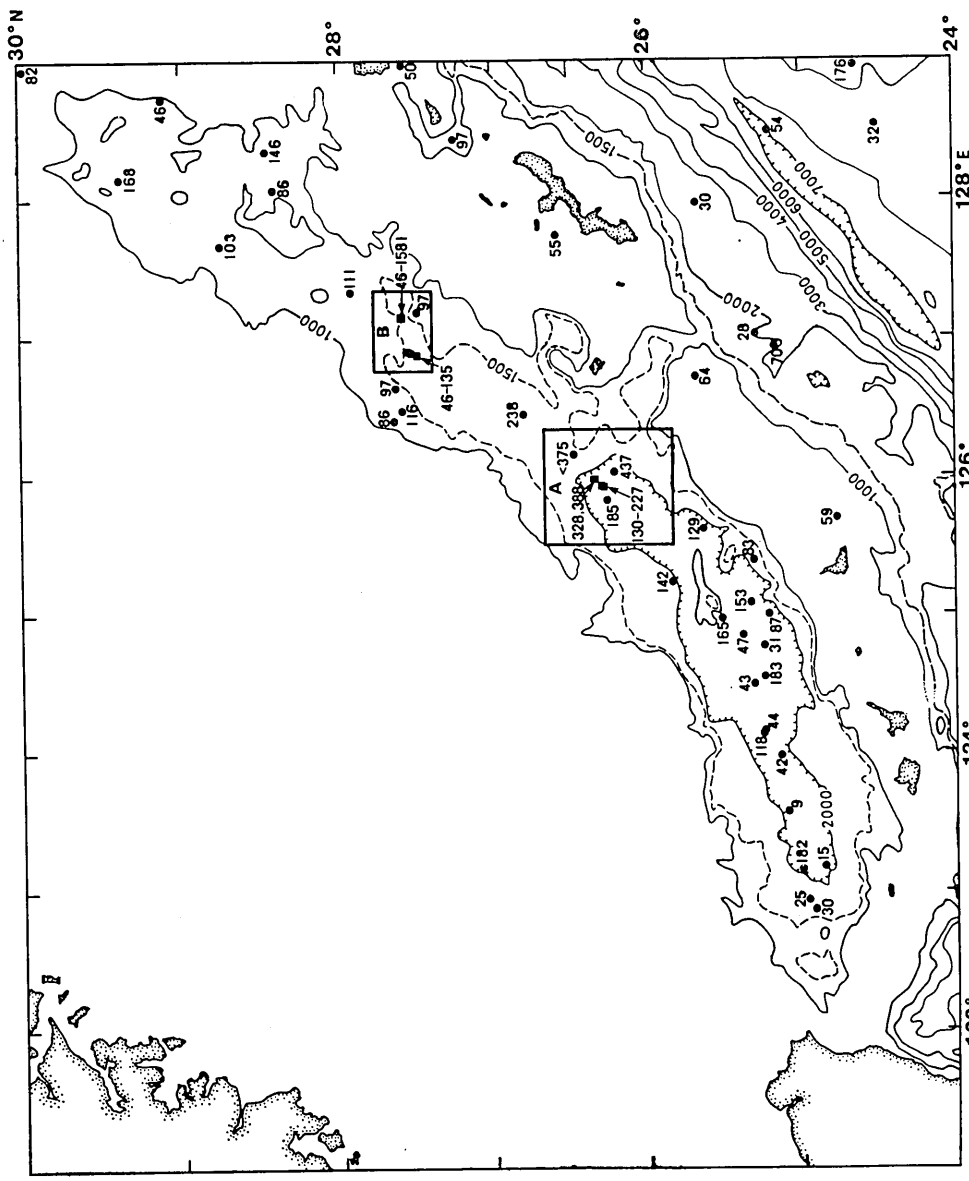

Fig. IV-10. Heat flow in the Okinawa Trough area (in mW/m²). Circles represent previous measurements and squares are the stations on this cruise. Sources of previous data are YOSHII (1979), LU *et al.* (1981) and HERMAN *et al.* (1978). Unpublished data by Lamont-Doherty Geological Observatory, Y. MATSUBARA, and K. SEKIGUCHI are also plotted. Detailed heat flow distributions in areas A and B are shown in Figs. IV-3 and IV-5.

The heat flow at HF6 is relatively low compared to other values reported in the middle Okinawa Trough (Figs. IV-5 and IV-10). If the flux of water inferred at HF6A and 6H is real, recharge and discharge of pore water may be occurring in the sedimented basin and the central ridge respectively. In such a case, most of the heat would be flowing out from the ridge.

At HF8 and 9, the heat flow is extraordinarily high except at HF9E, which is located at the northern margin of the Natsushima-84 Deep. In the oceans, heat flow values higher than 1000 mW/m^2 have been reported only in the Red Sea, on the Galapagos Spreading Center and in the Mariana Trough. High and variable heat flow suggests that hydrothermal circulations are occurring or there are very shallow heat sources such as magma chambers. Out of seven measurements in the deep, only two temperature profiles are non-linear and suggest the existence of hydrothermal flow. It is probable, however, that temperature profiles were non-linear but not detected at HF8B, 9A, and 9E because only two thermistors were active.

After this cruise, we made a more detailed heat flow survey in the Natsushima-84 Deep and obtained very high heat flow values of the same order accompanied by some non-linear temperature profiles (YAMANO *et al.*, 1986). Visual observations by the submersible SHINKAI-2000 were also made in the deep. Many fresh looking volcanic rocks were observed, with some indications of hydrothermal activity (UYEDA *et al.*, 1985).

References

BREDEHOEFT, J. D., and I. S. PAPADOPULOS, 1965, Rates of vertical groundwater movement estimated from the earth's thermal profile, *Water Resour. Res.*, **2**, 325-324.

BULLARD, E. C., 1954, The flow of heat through the floor of the Atlantic Ocean, *Proc. R. Soc. London, Ser. A*, **222**, 408-429.

CORLISS, J. B., J. DYMOND, L. I. GORDON, J. M. EDMOND, R. P. VON HERZEN, R. D. BALLARD, K. GREEN, D. WILLIAMS, A. BAINBRIDGE, K. CRANE, and T. H. VAN ANDEL, 1979, Submarine thermal springs on the Galapagos Rift, *Science*, **203**, 1073-1083.

HERMAN, B. M., R. N. ANDERSON, and M. TRUCHAN, 1978, Extensional tectonics in the Okinawa Trough, in *Geological and Geophysical Investigations of Continental Margins*, edited by J. S. Watkins, L. Montadert, and P. Dickerson, *Am. Assoc. Pet. Geol. Mem.*, **29**, 199-208.

HOBART, M. A., R. N. ANDERSON, and S. UYEDA, 1979, Heat transfer in the Mariana Trough, *EOS*, **60**, 383.

LISTER, C. R. B., 1972, On the thermal balance of a mid-ocean ridge, *Geophys. J.*, **26**, 515-535.

LU, R. S., J. J. PAN, and T. C. LEE, 1981, Heat flow in the southwestern Okinawa Trough, *Earth Planet. Sci. Lett.*, **55**, 299-310.

RATCLIFFE, E. H., 1960, The thermal conductivities of ocean sediments, *J. Geophys. Res.*, **65**, 1535-1541.

SIBUET, J-C., J. LETOUZEY, F. BARBIER, J. CHARVET, J-P. FOUCHER, T. W. C. HILDE, M. KIMURA, L-Y. CHIAO, B. MARSSET, C. MULLER, and J-F. STEPHAN, 1986, Tectonics in the Okinawa Through: constraints on backarc basin models of formation and evolution, submitted to *J. Geophys. Res.*

UYEDA, S., M. KIMURA, T. TANAKA, I. KANEOKA, Y. KATO, and I. KUSHIRO, 1985, Spreading center of the Okinawa Trough, *Tech. Rep. Japan Marine Science and Technology Center*, Special Issue "Deep Sea Research Using the Submersible 'SHINKAI 2000' System", 123-142 (in Japanese with English abstract).

VANDER ZOUWEN, D. E., 1984, Structure and evolution of Okinawa Trough, *M. Sc. thesis*, Texas A and M Univ. 130 p.

VON HERZEN, R., and A. E. MAXWELL, 1959, The measurement of thermal conductivity of deep-sea sediments by a needle-probe method, *J. Geophys. Res.*, **64**, 1557-1563.

YAMANO, Y., S. UYEDA, Y. FURUKAWA, and G. A. DEHGHANI, 1986, Heat flow measurements in the northern and middle Ryukyu arc area on R/V Sonne in 1984, *Bull. Earthq. Res. Inst. Univ. Tokyo*, **61**, 311-327.

YOSHII, T., 1979, Compilation of geophysical data around the Japanese islands (I), *Bull. Earthq. Res. Inst., Univ. Tokyo*, **54**, 75-117 (in Japanese with English abstract).

DELP 1984 年度中部沖縄トラフ研究航海報告
IV. 地殻熱流量測定

東京大学地震研究所 山野　誠
東京大学地震研究所 上田誠也
千葉大学理学部 木下　肇
Texas A and M 大学 Thomas W. C. HILDE

沖縄トラフ中部の3地域において，地殻熱流量測定を実施し，計17点で新たに熱流量値を得た．温度勾配の測定には，Columbia 大学 Lamont-Doherty 地質学研究所製の Ewing 型の測器を用いた．この測器は多重挿入が可能で，音響パルスにより船上へデータを伝送する能力を持つ．堆積物の熱伝導率は，グラビティ・コアラーによって採取した試料について熱線法で測定した．非線形の温度勾配が得られた地点では，これを堆積物中の間隙水の移動によるものと解釈して熱流量を求めた．

東経126度付近は従来高熱流量地域であるとされていたが，今回の測定でもいずれも 130 mW/m² を越える高い値が得られた．東経127度付近のトラフ中軸部では，東西に延びる小海嶺の南北と，その東に存在する"なつしま84海凹"と呼ばれる小凹地の中で測定を行った．海嶺の近辺では比較的低い値が観測されたのに対し，"なつしま84海凹"においては最大約 1600 mW/m² に達する異常な高熱流量が得られた．熱流量が非常に高くてばらつきが大きいことは，この凹地付近で熱水活動が起こっている可能性を示唆している．